

PGC 60020: a Polar-Ring Galaxy

O.A. Merkulova^{1, a}, G.M. Karataeva^a, V.A. Yakovleva^a, and A.N. Burenkov^b

^aAstronomical Institute of Saint-Petersburg State University

^bSpecial Astrophysical Observatory, Russian Academy of Sciences

Abstract

We present an analysis of new observations of a peculiar galaxy PGC 60020, obtained with the 6-m BTA telescope of the SAO RAS with a multimode SCORPIO instrument. The observational data includes direct images in the B, V, R_c photometric bands and long-slit spectra in the red range (the H_α line spectral region). Based on the analysis of these data it was found that PGC60020 belongs to the type of classical polar-ring galaxies. Its main body is an S0 galaxy, around the major axis of which a disk of gas, dust and stars is rotating in the plane inclined at an angle of about 60° to the galactic plane. A loop-shaped structure stretches from the southern part of this disk (possibly, a tidal tail) towards the SDSS J171745.58+404137.1 galaxy.

Key words: galaxies: peculiar—galaxies: structure—galaxies: individual: PGC 60020—galaxies: individual: SDSS J171745.58+404137.1

1 Introduction

Polar-ring galaxies (PRG) are a rare class of dynamically peculiar systems, where a ring or a disk consisting of gas, dust and stars is rotating around the major axis of the main body near the polar plane [1]. It is believed that such polar structures can emerge either from the interaction or even a merger of galaxies, or as a result of accretion of gaseous filaments from the intergalactic medium to the main galaxy ([2–4], etc.). The unique geometry of PRGs allows to obtain the data on the three-dimensional distribution of the central galaxy's potential and about the dark halo [5–7], which only increases the interest to these objects.

The catalog of PRGs and related objects by Whitmore et al. [1], based on the photographic images includes 157 galaxies. To date, the existence of kinematic systems, rotating in different planes (classical PRGs) is confirmed only in about two dozen of them. A small number of known objects does not yet allow to make more or less definite conclusions about their nature,

¹E-mail: olga_merkulova@list.ru

evolution, and the properties of the dark halo. Therefore, the search for answers to many issues related to the emergence, stability and age of polar rings (PR) is still pertinent. More comprehensive and accurate data on the kinematics of the stellar and gaseous components, the properties of the stellar population and interstellar medium, the processes of star formation is needed. The discovery of new objects of this class and their detailed study is of great interest indeed.

An important step in this direction was the publication of a new catalog of PRG candidates by Moiseev et al. [8] in 2011. This catalog is created based on the results of the Galaxy Zoo project², where the volunteers performed a visual classification of nearly a million galaxies from the Sloan Digital Sky Survey (SDSS³). Based on the preliminary classification of the Galaxy Zoo and visual inspections of more than 40 000 images from the Sloan survey, Moiseev and his colleagues have selected 275 galaxies and compiled their own Sloan-Based Polar Ring Catalog (SPRC). Using the spectral data, obtained both by the authors of the SPRC catalog and other groups of researchers (see the references in [8]), the existence of kinematic systems, rotating in different planes has already been confirmed for about 10 galaxies from this catalog.

This paper is devoted to the spectral and photometric investigation of the PGC 60020 galaxy. In appearance, this galaxy is similar to the PRGs. This was first noticed by I. D. Karachentsev (SAO RAS). He suggested that it belongs to the PRG class of objects and kindly offered to include PGC 60020 in the program of our research of the PRG candidates. The first spectral observations of this galaxy, performed at the 6-m BTA telescope of the SAO RAS in 2008 have confirmed the existence of two kinematic gaseous subsystems, one of which is related to the main body of the galaxy, and the other one—to the suspected PR [9]. Judging on its external features, PGC 60020 was included in the new SPRC catalog under the number SPRC-67 as a possible PRG candidate. We present the results of our observations of PGC 60020 and their discussion in this paper. The next section gives a brief about the instruments the observations were made with, and the data processing method. Further, sections 3 and 4 present the results of our study of the morphology and kinematics of PGC 60020. The conclusion discusses all the results we obtained.

2 Observations and processing

The observations of the PGC 60020 galaxy were performed at the 6-m BTA telescope of the Special Astrophysical Observatory of the Russian Academy of Sciences (SAO RAS). The EEV 42-40 CCD, sized 2048×2048 pixels (after the 2×2 averaging the pixel size amounted

²<http://www.galaxyzoo.org/>

³<http://www.sdss.org/>

to $0.''357 \times 0.''357$) was used as a radiation detector.

The photometric observations of the galaxy in the Johnson B and V bands and Cousins R_c -band were made with the SCORPIO multi-mode focal reducer [10], mounted at the primary focus between May 20 and 21, 2010. Standard stars from the list of Landolt [11] were observed for calibration overnight. The data on the photometric observations are given in Table 1. The

Table 1: Photometric observational data for PGC 60020

Band	Exposure time, frames \times s	Seeing, arcsec	z, deg
B	4×350	2	10–14
V	5×180	2	15–17
R_c	11×60	1.8–2.2	7–9

observational data reduction was carried out using the ESO MIDAS software package. Correcting for the atmosphere, we used the mean transparency coefficients of the BTA location [12]. The accuracy of measurement of the integral magnitude of the galaxy amounts to $\pm 0.^m1$.

Spectral observations were also carried out in the primary focus of the 6-m telescope with the SCORPIO focal reducer in the long slit spectral observations mode, using the VPHG1200R grism; the slit width amounted to $1''$, the scale along the slit was $0.''357/\text{px}$, and spectral resolution amounted to 5\AA . The log of observations is presented in Table 2.

Table 2: Spectroscopic observational data for PGC 60020

Date	Exposure time, frames \times s	Seeing, arcsec	Spectral region, \AA	PA, deg
27.07.2008	2×1200	1.6	5700–7400	115
27.07.2008	2×1200	2.4–1.6	5700–7400	–10
19.07.2010	5×1200	1.7	5700–7400	115
20.07.2010	8×1200	1.2	5700–7400	–10

The observations in the long slit mode were performed in 2008 and 2010 in the red spectral range, containing the following emission lines: H_β , $[\text{NII}] \lambda\lambda 6548, 6584\text{\AA}$. The reduction of the obtained data was carried out using the standard procedures within the ESO MIDAS environment. After the primary reduction, to increase the signal-to-noise ratio we summed all the obtained spectra, and the resulting spectrum was smoothed along the slit by a 3-pixel-high rectangular window. The radial velocities of the gas component were measured by

the positions of the centers of Gaussians, inscribed into the emission lines. The accuracy of these measurements was estimated by the night sky [OI] λ 6300Å line and amounted to 10–15 km/s. The cross-correlation method [13] was applied to determine the radial velocity from the absorption lines.

3 Multicolor photometry results

3.1 Features of the photometric structure in PGC 60020

The photometric observations of PGC 60020 were obtained in three filters, B, V, R_c . The image of the galaxy in the R_c -band is given in Fig. 1a. Its main body has a lenticular shape: a bright ellipsoidal central region and a faint external disk, visible at an angle to the sky plane. By appearance, this galaxy can be attributed to the S0 morphological type, although the LEDA database designates it as an elliptical with a question mark (E?). To the north and south of the galactic plane along the -10° direction, extended luminous regions are visible, the presence of which makes PGC 60020 very similar to such classic PRGs as NGC 2685, ESO 415-G26, IC 1689, and AM 2020-504 [4, 14–16]. A comparison of direct images obtained at the 6-m telescope with the SDSS images has shown that the BTA images are deeper, hence only our data were used in the analysis of the external structure of the galaxy.

The outer regions of the main body and the suspected PR are very faint. We summed the frames, obtained in three filters, the total image is shown in Figs. 1b and d, where the features of the outer regions of PGC 60020 and its immediate surroundings are more discernible. In the vicinity of PGC 60020 (in a circle of a $1'$ radius) three faint galaxies are observed. Visually inspecting the total B+V+ R_c image with the superimposed isophotes (Fig. 1d) one gets an impression that from the southern end of the suspected PR a luminous arc stretches to one of these objects, located at a distance of $22.''2$ to the south-east from the PGC 60020 center. This object is identified as the SDSS J171745.58+404137.1 galaxy. However, to date, neither its morphology, nor redshift are known. For the other two faint galaxies such data are also absent. The presence of a luminous arc between PGC 60020 and SDSS J171745.58+404137.1 allows to suspect that the latter belongs to the close neighborhood of PGC 60020, and further in this paper we shall call the given object a “companion” galaxy.

To clarify the structural features of PGC 60020, the unsharp masking image manipulation technique was applied, where the Gaussian smoothing was performed with a $\sigma \approx 7''$ window of the studied galaxy. Figure 1c presents a mask, obtained after subtracting the smoothed image in the R_c filter from the initial image. It is clear that the main body of the galaxy consists of a bright bulge and an inclined disk, and that the diameters of the major axes of the galaxy and

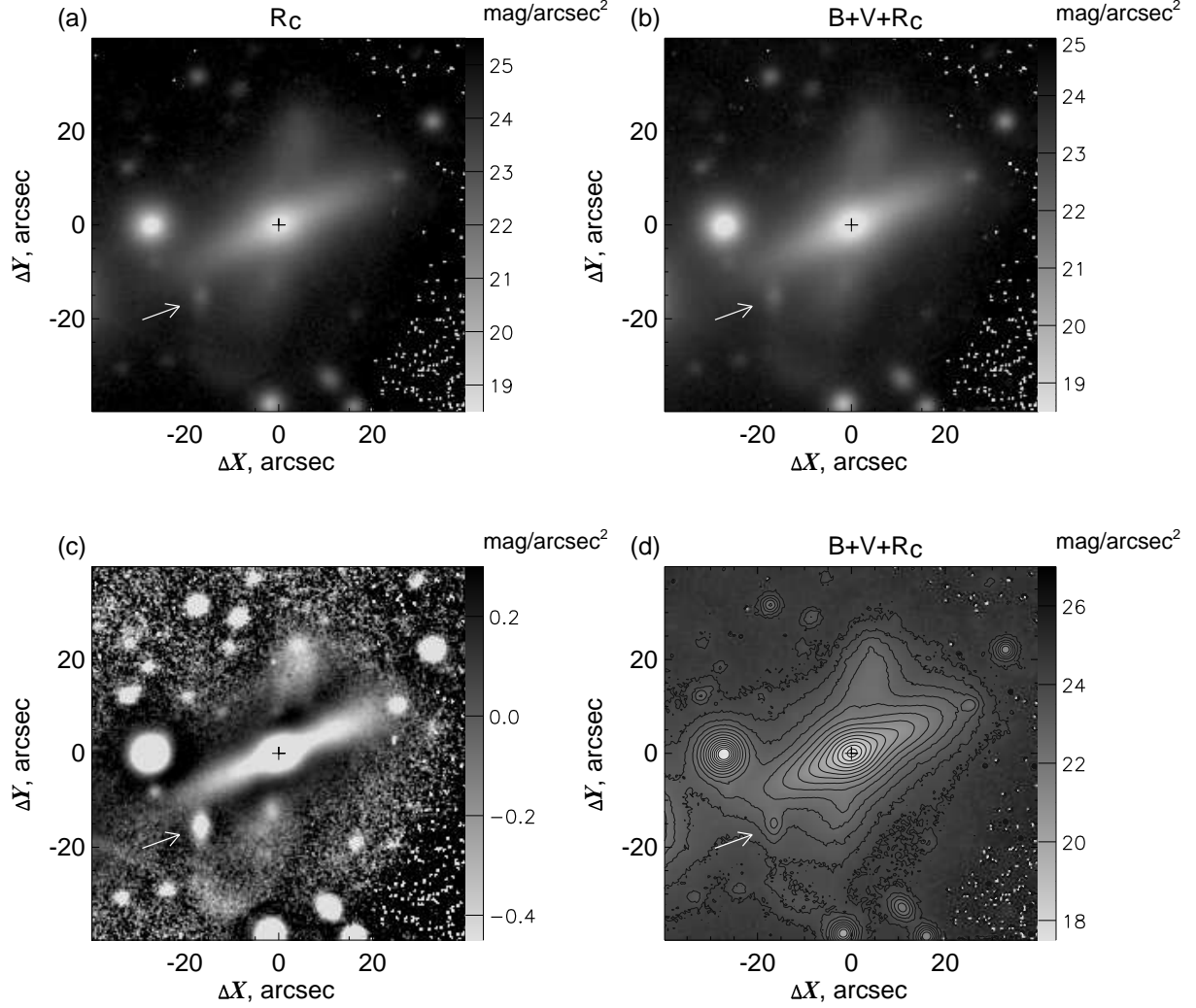


Figure 1: PGC 60020 and its companion galaxy SDSS J171745.58+404137.1: (a) the image in the R_c -band; (b) the total image in the B, V, R_c -bands; (c) the residual image in the R_c -band, obtained by subtracting the image, processed by a median filter; (d) the total image in the B, V, R_c -bands with the isophote contours. N is on top, E is on the left. An arrow points to the SDSS J171745.58+404137.1 galaxy.

the suspected ring are about the same (the outer parts of the ring extend up to nearly $20''$ from the center). The companion galaxy is roughly elliptical in shape. In this image, the luminous arc, mentioned above is clearly discernible.

Figure 2 presents the isophotes of PGC 60020 in the B, V, R_c -bands and the photometric sections along the major axes of the main body and the ring. The shape of the isophotes in all colors is about the same. It should be noted that the presence of the ring greatly distorts the shape of the outer isophotes of the main body of PGC 60020. For the analysis of the photometric structure, we used the technique, based on the Fourier series expansion of the isophote deviation from elliptical, suggested in [17].

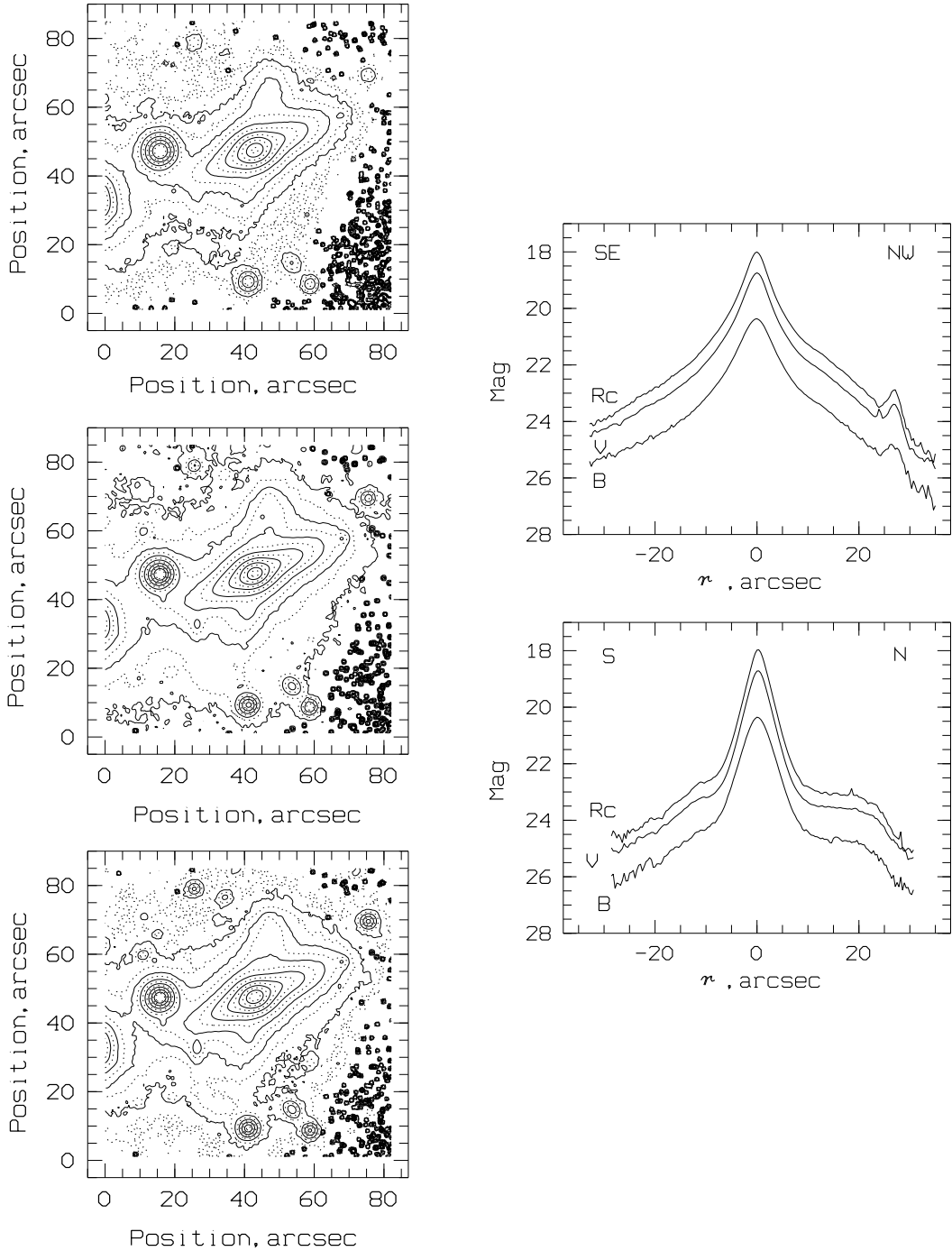


Figure 2: PGC 60020: left column (from top to bottom): the galaxy isophotes in the B, V, R_c -bands (in increments equal to $0.^m5/\square''$; the outer isophote in the B-band corresponds to the surface brightness of $26.^m5$, in the V-band— $25.^m5$, and in the R_c -band— $25.^m5$; N is on top, E is on the left); right column: the B, V, R_c image sections along the major axes of the main body (top) and the ring (bottom).

The isophote analysis (of the frames in the B and R_c -bands) was performed in the IRAF environment. For each value of the major axis (a) we computed the ellipticity (ϵ_{ell}) and the position angle of the major axis of the inscribed ellipses (PA_{ell}), which was measured from the

direction to north towards east, as well as the dimensionless coefficients of the third and the fourth harmonics in the Fourier series expansion. The difference between the coefficients of these harmonics, especially the third one, in the B and R_c -bands is a reliable indicator of the presence of dust in the galaxy [18]. The findings of this analysis are presented in Fig. 3.

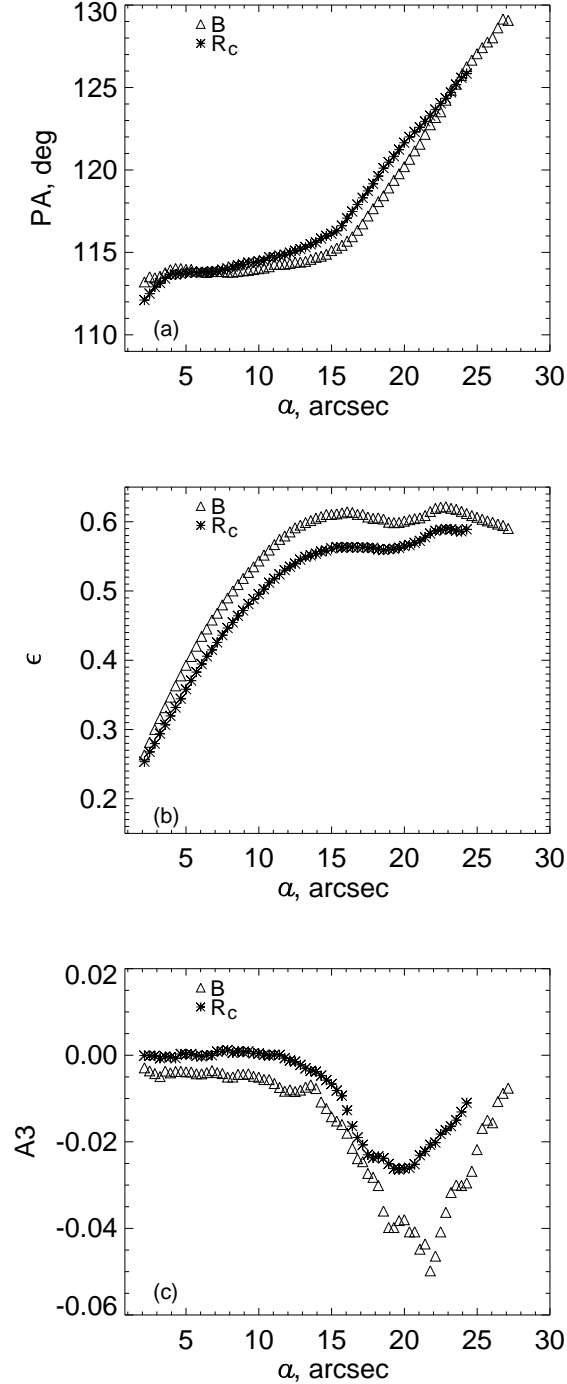


Figure 3: PGC 60020: the characteristics of the isophote shapes in the B (triangles) and R_c (asterisk) bands, depending on the semi-major axis of the ellipse, inscribed in the isophote: (a) position angle, (b) ellipticity, (c) the coefficient of the third harmonic A_3 .

Overall, the behavior of the ϵ_{ell} and PA_{ell} ellipse parameter variability in both filters is about the same (Fig. 3a and b). In the interval from $2''$ to $15''$ the ellipticity smoothly varies from 0.25 to about 0.56 in the R_c filter, and up to 0.60 in the B filter, while at large distances it is approximately constant. In the galactic region from $4''$ to $16''$, PA_{ell} varies little and on the average $PA_{ell} = 115^\circ$. Further, a variation of the position angle is observed, and at the distance of $24''$, $PA_{ell} \approx 125^\circ$. Such a variation of PA_{ell} is most likely due to the fact that at these distances, the surface brightness of the ring becomes comparable to the surface brightness of the main body of PGC 60020. In this case, the shape of the outer isophotes gets distorted, and the position angle of the major axis of the galaxy itself (PA_{gal}) does not vary (see Fig. 2).

In the central region of the galaxy ($a \leq 10\text{--}15''$) the coefficients of the cosine and sine of the third and fourth harmonics (A3, A4, B3, B4) are close to zero in both filters, then their values become nonzero, but the differences in the B and R_c filters are observed only in the A3 coefficient. Figure 3c shows that up to $a \approx 15''$ the value of A3 is approximately equal to zero. Further, it becomes negative, and a little difference emerges between the filters, amounting to 0.02–0.03. Based on this we can conclude that the main body of the galaxy is poor in dust, though a small amount of dust may be present in the ring.

As a result of studying the photometric structure of PGC 60020, we have taken that the position angle of the major axis of the galaxy $PA_{gal} = 115^\circ \pm 2^\circ$, and the angle of inclination of the disk plane to the sky plane $i_{gal} = 65^\circ \pm 2^\circ$. The ellipticity ϵ was taken to be 0.56 (the value obtained in the R_c -band), since in the analysis of the galaxy image in the K_s -band from the Two-Micron Sky Survey (2MASS), the value of ϵ proved to be closer to the ellipticity measured in the R_c -band. The position angle of the major axis of the ring is $-10^\circ \pm 2^\circ$, and the angle of inclination to the plane of the sky is approximately $79^\circ \pm 5^\circ$ (the ellipticity is 0.8). Knowing the inclination of the disk plane of the main body of the galaxy and the ring to the sky plane (65° and 79° , respectively) and the positions of their major axes (115° and -10° , respectively), we can find the angle between the disk and the ring from the expression:

$$\cos \Delta i = \pm \sin i_1 \sin i_2 \cos(PA_1 - PA_2) + \cos i_1 \cos i_2,$$

where i_1, i_2 are the disk and ring inclination angles to the sky plane, PA_1, PA_2 are the position angles of the major axes of the galactic disk and the ring. This angle was found to be $54^\circ \pm 4^\circ$ and $115^\circ \pm 4^\circ$.

In conclusion, let us say a few words about the structure of the companion galaxy. Its surface brightness is low, the images in all filters are amorphous, without any features. As noted above, it is elliptical in shape. The scale of the major axis of the ellipse in the B-band from the $\mu_B = 25.0 \text{ mag}/\square''$ isophote is about $4.''3$, the ratio of the semiaxes amounts to about 0.56, and the ellipticity is approximately 0.4. This value corresponds to the ellipticity of E4–E5 galaxies.

3.2 Photometric properties of galaxies

Apparent integral magnitudes and color indices of the PGC 60020 galaxy and its companion were determined using the multiaperture photometry [19] with the accuracy of $\pm 0.^m1$, as stated above. The integral values, corrected for the extinction in our Galaxy [20] are listed in Table 3. The apparent magnitude of PGC 60020 that we obtained, $B_{t,0} = 15.^m6$ coincides with the value

Table 3: Main characteristics of PGC 60020 and the suspected companion galaxy

Characteristics	PGC 60020	Companion
Morphological type	E?*	–
	S0	E4-E5
Distance ($H_0 = 72$ km/s/Mpc)	118 Mpc	–
Scale	0.57 kpc in 1''	–
V_{gal} , km/s	$8507 \pm 60^{**}$	–
	8489 ± 20	–
Semi-major axis a ($\mu_B = 25.0$)	23.8'' (13.6 kpc)	4.3''
Position angle of the major axis PA_{gal}	115°	0°
Inclination angle i_{gal}	65°	–
Semi-major axis of the ring a_{ring} ($\mu_B = 25.0$)	21.4'' (12.2 Kpc)	–
Position angle of the ring's major axis PA_{ring}	–10°	–
Inclination angle of the ring i_{ring}	79°	–
$B_{t,0}$, mag	15.6	17.7
(B–V) ₀ , mag	1.15	1.06
(V–R) ₀ , mag	0.58	0.47
M_B , mag	–19.9	–
B/D	0.6	–

* The data adopted from the HyperLeda database (<http://leda.univ-lyon1.fr/>),

** The data adopted from the NED database (<http://ned.ipac.caltech.edu>)

given in the LEDA database within the limits of error. Calculating the absolute magnitude M_B , we have introduced a correction for redshift. The integral B–V color index of PGC 60020 is by about $0.^m2$ redder than the average color index of the early-type galaxies. As shown above, this fact can not be explained by the presence of dust. Regarding the value of V–R_c, we can assume that within the errors its value coincides with the color indices of E–S0-type galaxies. Since a major part of the ring is projected on the main body of the galaxy, its luminosity can not be reliably estimated. We can only find the apparent integral magnitude of two prominent

luminous regions located to the north and south of the main body of the galaxy. Their integral magnitude is about 19^m , which is about 4% of the total luminosity of PGC 60020.

Integral color indices of the companion are similar to the indices of elliptical galaxies within the limits of error.

The distributions of B–V and V–R_c color indices, as well as the B–V and V–R_c sections along the major axes of the main body and the ring are demonstrated in Fig. 4. The reddest

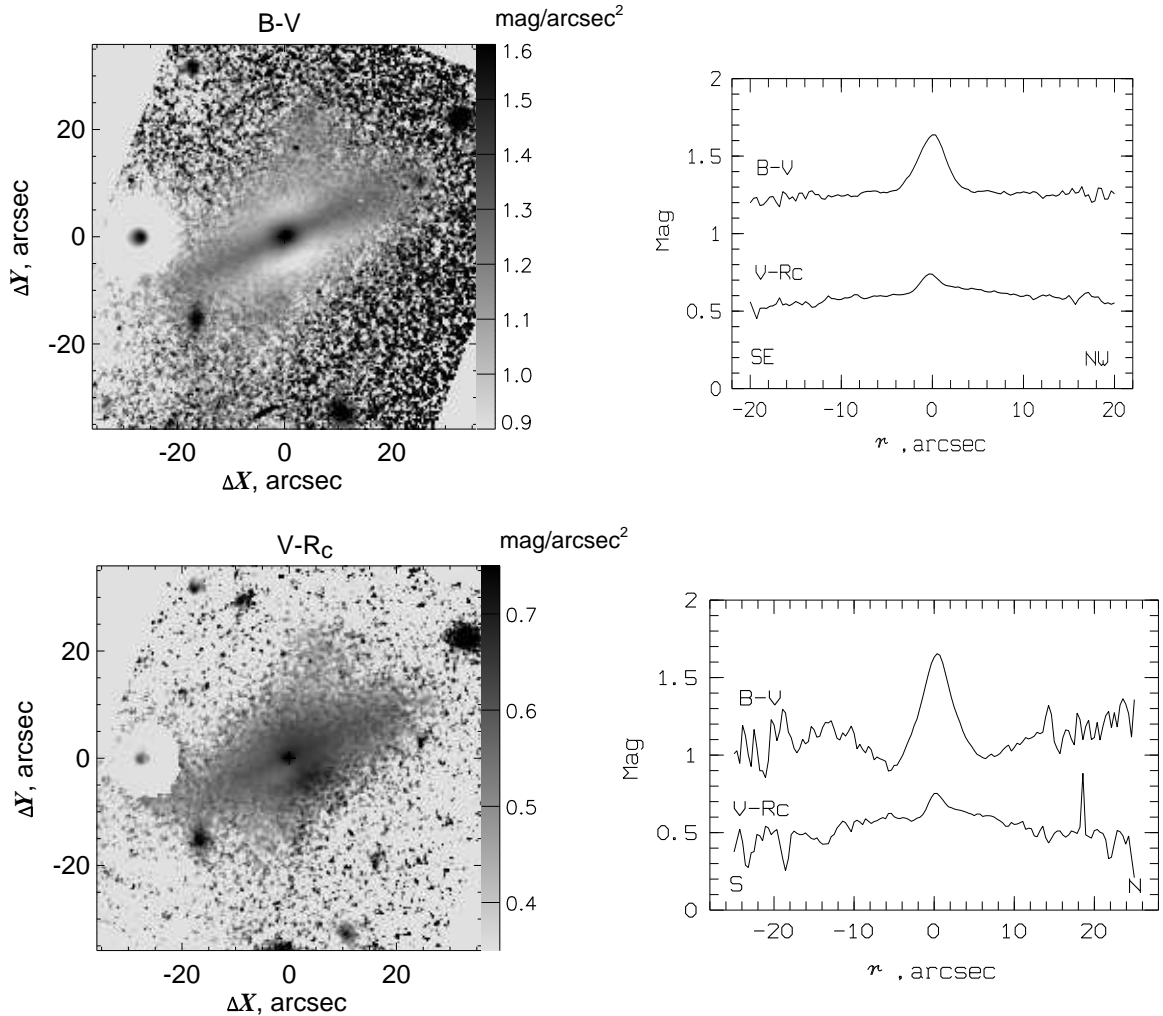


Figure 4: PGC 60020: left column: the B–V (top) and V–R_c (bottom) distributions (N is on top, E is on the left); right column: the B–V and V–R_c sections along the major axes of the main body (top) and the ring (bottom).

color indices B–V are observed in the circumnuclear region ($r < 2\text{--}3''$) of PGC 60020 and in the center of the companion galaxy, where B–V reaches $1.^m6$ and about $1.^m5$, respectively. In the plane of the disk of PGC 60020, the value of B–V is constant within the error limits and amounts to $1.^m2 \div 1.^m3$. The color index decreases with distance from the galactic nucleus, while in the direction to NE and SW at the distance of approximately 4–5'' two regions with $B-V = 0.^m8 \div 0.^m9$ are observed, of which the SW region is more extended. It extends approximately in parallel to the galactic plane, and its size in this direction is about 12–14''.

The distribution of the $V-R_c$ color index is more uniform, and the value of $V-R_c$ changes little: from about $0.^m7$ in the nucleus of PGC 60020 to $0.^m5$ on the periphery. As for the companion, its $V-R_c$ color stays almost constant and is equal to about $0.^m7$.

In the region of the ring, the color indices bluer than in the main body of the galaxy are observed ($B-V \approx 0.^m9-1.^m0$). A considerable scatter of $B-V$ values at the section along the major axis of the ring (Fig. 4, bottom right plot) at $r > 16''$ is explained by a clumpy structure of the ring and a deterioration in accuracy due to the low surface brightness. At the distance of approximately $5-6''$ to the north and south from the center, where the given section crosses two blue regions, whose existence was mentioned above, a decrease of $B-V$ is observed, while from the south this effect is more noticeable. In general, it should be noted that the color indices of the ring are by about $0.^m2-0.^m3$ higher than the color indices of the rings in classic PRGs (see, e.g., [4]).

Figure 2 (right column, at the top) shows the sections along the major axis of the galaxy in three filters. For the decomposition into components, we used the B-band section along the major axis. We can isolate two areas in this section: the central area (up to $r \approx 7''$ from the center) with a steeper profile and an extended external area ($10'' \leq r \leq 25''$), where the profile is less steep. The brightness profile in the outer region almost throughout its length is well represented by an exponential law with a scale factor $h_d = 8.^m2$ (4.7 kpc) and central surface brightness $\mu_d = 21.9 \text{ mag}/\square''$ (Fig. 5a). The central structure (the bulge) can be described by the de Vaucouleurs law with an effective radius $R_{e,b} = 1.^m4$ (0.8 kpc) and effective surface brightness $\mu_{e,b} = 20.03 \text{ mag}/\square''$.

Using the found parameters of the bulge and the disk a two-dimensional model of the galaxy was constructed. At that, we assumed that the position angle of the photometric axis amounts to 115° , and the inclination of the bulge and the disk of PGC 60020 to the sky plane is 65° . The residual brightness distribution, obtained by subtracting the two-dimensional model from the galaxy image in the B-band is shown in Fig. 5b. It clearly demonstrates an increase of differences between the observed and model brightness distributions in the region of the ring.

We also estimated the total luminosity ratio of the bulge and the disk B/D. It was found to be 0.6, a value typical of S0 or Sa galaxies [21].

4 Results of spectroscopic observations

Long-slit spectra of PGC 60020 were obtained along the major axes of the main body ($PA = 115^\circ$) and suspected ring ($PA = -10^\circ$). Both spectra show a high-energy continuum with strong absorption lines of the NaI D $\lambda 5890, 5896 \text{ \AA}$ doublet and the blend of FeI+CaI+BaII lines around $\lambda 6495 \text{ \AA}$. Among the emission lines, the [NII] and [SII] doublets are present, as well as the H_α

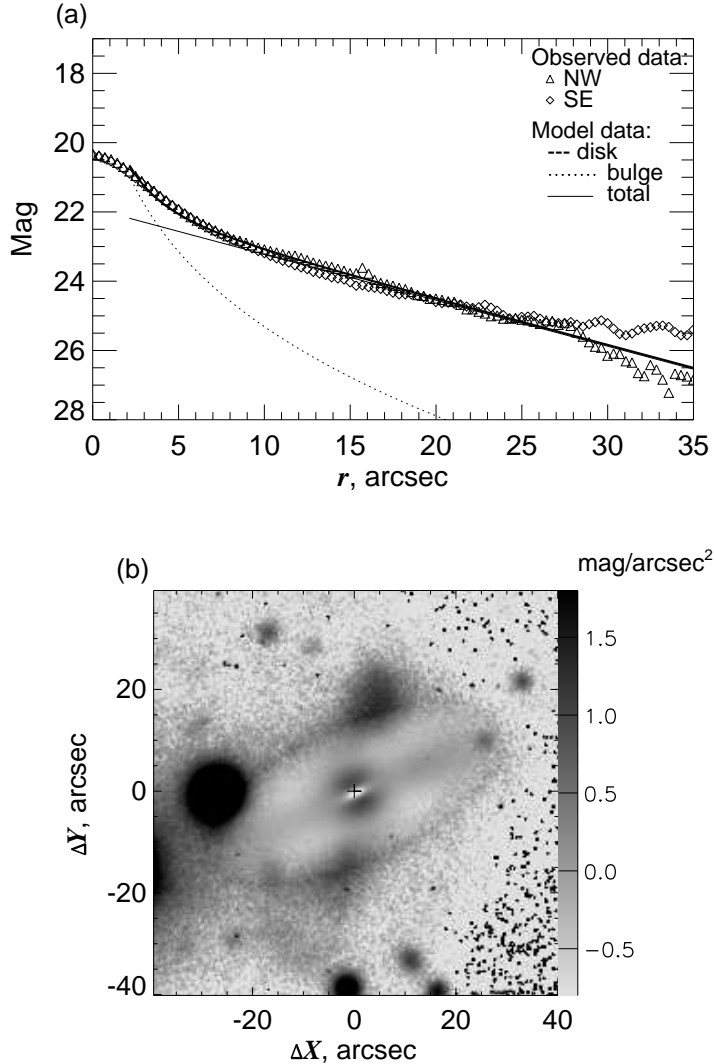


Figure 5: PGC 60020: (a) the observed brightness profile along the major axis with $\text{PA} = 115^\circ$ and its decomposition into components; (b) residual image after subtracting the two-dimensional model from the B-band image.

line. However, in our spectra the [SII] lines of the object fall on the lines of the sky, the line of H_α in the emission is superimposed over a strong absorption line, and the [NII] 6548 \AA line can be reliably identified only in the nuclear region ($r < 2''$), sinking in the noise at large distances from the center. Therefore, the radial velocity curves were built based on the [NII] $\lambda 6584 \text{ \AA}$ line.

To construct the stellar radial velocity curves using the cross-correlation method, the spectrum of the galactic nucleus was used, since the spectra of template stars were not be obtained. We succeeded in constructing the curves of stellar radial velocities along the major axis of the galaxy ($\text{PA} = 115^\circ$), and along $\text{PA} = -10^\circ$ up to the distances of $r = 8\text{--}10''$, and about $4''$ from the center, respectively (Fig. 6). These curves do not manifest any specific features, they are typical of galactic disks: the maximum velocity gradient along the major axis of the

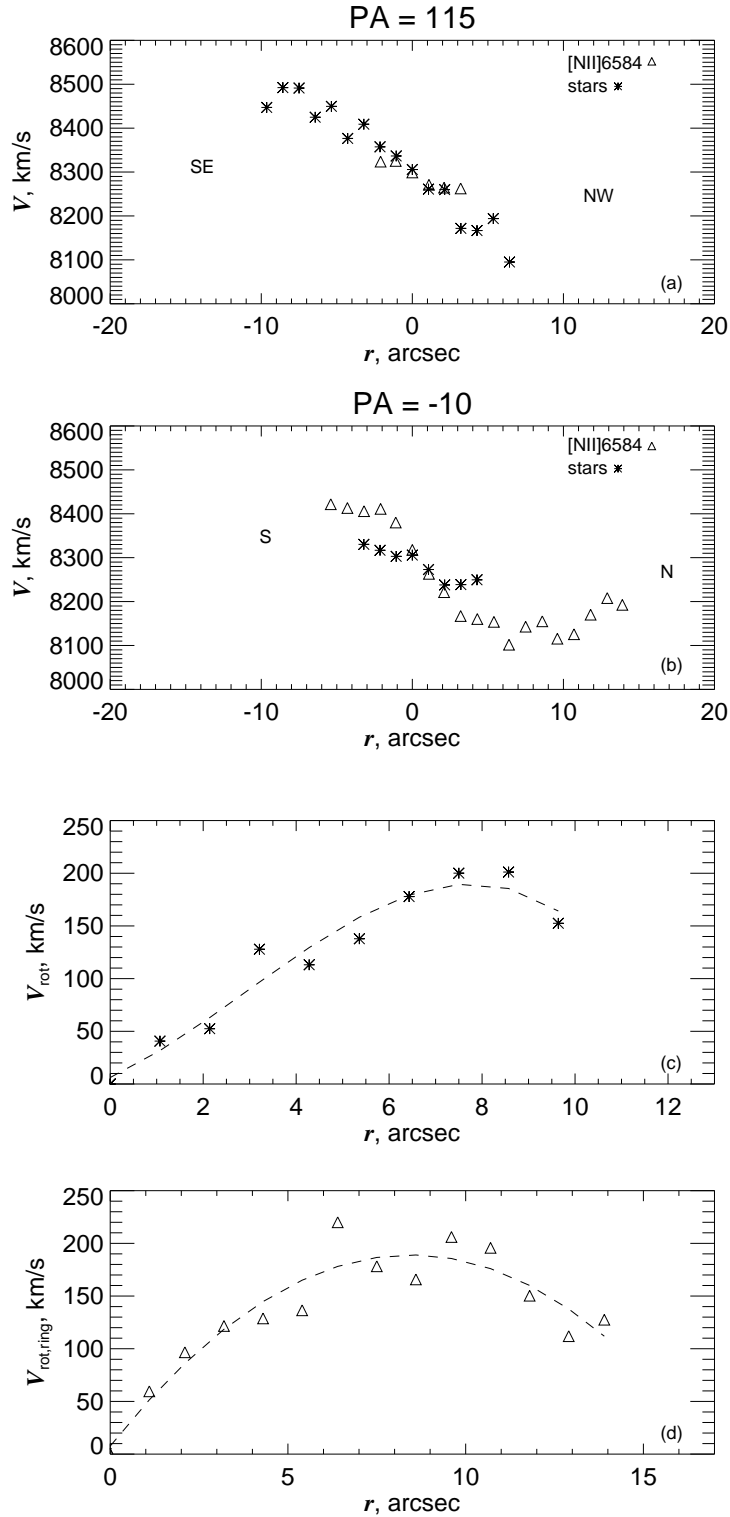


Figure 6: PGC 60020: radial velocity curves of ionized gas and stars along the major axes of the main body (a) and the suspected ring (b); rotation curves of the main body stellar component (c) and ionized gas of the ring (d). The signs (the asterisks and triangles, respectively) mark the observed rotation curves, and the dashed lines—the average smoothed rotation curves.

disk and a small velocity gradient along the direction between the major and minor axes (PA = -10°). Assuming that the stars rotate in circular orbits, and given the inclination of the main body to the sky plane (65°), we recalculated the curve of stellar radial velocities of stars along PA = -10° to the curve along the major axis. Both curves coincided within the error of observations. This means that the absorption lines in the spectra along PA = 115° and -10° belong to the stellar population of the main body of the galaxy. If we assume that the photometric axis of the main body coincides with the dynamic axis, we can then construct in the region up to $r \approx 10''$ the rotation curve of the galaxy (Fig. 6c). The velocity gradient in the rectilinear section is about 44 km/s/kpc. It is possible that at a distance of $R_{max} = 8''-10''$ (4.6–5.7 kpc) the rotation curve reaches a plateau, and then the maximum velocity amounts to approximately 200 km/s. The estimate of the mass, enclosed within the radius of R_{max} yields the value of $M(R_{max}) \geq 4.3 \times 10^{10} M_\odot$.

The radial velocity curves of ionized gas are shown in Fig. 6. Note that in the circumnuclear region of the galaxy the full width at half maximum (FWHM) of the [NII] $\lambda 6584 \text{ \AA}$ line is about 460 km/s. Along the major axis of the main body, this line is visible only in the circumnuclear region ($r \leq 3-4''$). A similar pattern is observed in some classical PRGs, for example, in NGC 2685 [22]. The radial velocity gradient along the major axis is about 33 km/s/kpc (Fig. 6a). Since the central region of the galaxy does not reveal any features, we can assume that the photometric and dynamical centers coincide, and the heliocentric velocity of the galactic center is about 8308 ± 20 km/s. The radial velocity gradient of ionized gas along the major axis of the galaxy proved to be slightly lower than the velocity gradient in the rectilinear region of the stellar radial velocity curve.

The line of nitrogen can be traced from the northern part to $14''$ from the center, and from the southern part only to $7''$ along the major axis of the ring. This result is not surprising, since the northern part of the ring is much brighter than its southern counterpart (see Fig. 1a). The radial velocity curve along the major axis of the ring demonstrates that the gas of the disk is rotating around the major axis of the main body of the galaxy. In the central region with the $r \approx 3''$ radius there is a straight section with a velocity gradient of approximately 81 km/s/kpc. Farther off, the velocity gradient declines, and in the northern part the radial velocity curve reaches a plateau. At a distance of $r \approx 8''$ the peak radial velocity is reached with respect to the system center, amounting to approximately -170 km/s, then it decreases to come up to about -120 km/s at $r \approx 13''$.

A large velocity gradient in the rectilinear region of the curve indicates that the polar structure, observed in PGC 60020 is evidently a *polar disk*, and the emission of ionized gas, belonging to this disk, makes a significant contribution to the total emission of gas in the central region of the galaxy. This also explains a smaller radial velocity gradient of ionized gas relative

to the gradient of radial velocity of stars along the major axis of the galaxy (Fig. 6a). Further in the text we shall use the term “polar disk” instead of the “polar ring”. Figure 6d shows the observed rotation curve of ionized gas in the polar disk, constructed in the assumption that the gas is rotating in circular orbits, the position angle of the disk’s major axis is -10° , and its angle of inclination to the sky plane is 79° . The peak velocity is reached at about the same distances from the center, as those revealed in the rotation curve of the stellar component of the main body of the galaxy, and is about 190 km/s.

We have also attempted to obtain the spectrum of the companion galaxy (the observing set of May 15 to 16, 2012) in order to determine its redshift. However, the object is faint and due to bad weather conditions the obtained spectrum has revealed the stellar continuum only, resulting in the failure to estimate the redshift of SDSS J171745.58+404137.1.

5 Discussion and conclusions

Before the final conclusions, let us discuss some features of the PGC 60020 galaxy, discovered in the course of our research. The characteristics we have determined are presented in Table 3.

It was earlier noted that in some aspects the main body of the galaxy can be attributed to the S0 type, however, its integral color indices proved to be redder than those typical of the elliptical galaxies, and even more so than in the classical PRGs with S0-type main bodies. The analysis of the isophote shapes in the B and R_c -bands did not reveal any presence of dust in the main body of the galaxy. Consider other possible explanations of this feature.

One reason may be due to the fact that PGC 60020 is poor in gas. This is confirmed by the presence of emission lines only in its central region ($r \leq 3-4''$), where the total emission of ionized gas of the polar and galactic disks is observed. Moreover, the outer parts of the galactic disk do not reveal any noticeable decrease in the color indices, typical of the majority of classical PRGs.

On the other hand, the redder color indices may be possibly related with the features of stellar population in the circumnuclear region of the galaxy. Large B–V color indices, reaching $1.^m6$ in this region, and a powerful continuum with strong absorption lines imply the presence of a large number of late-type stars. However, we are currently not in possession of the data required to perform the study of stellar populations (age, metallicity). We consider unreliable the use of color indices in the case of such a peculiar galaxy as PGC 60020 for such an analysis. To make the final conclusions, high quality spectra with a good spectral resolution are required for the absorption line analysis.

Two areas with bluer indices are visible in the distribution of B–V color indices (see Fig. 4, top left plot) towards the NE and SW of the galactic center at a distance of about 4–5''. Blue

color indices are most likely related to the fact that the polar disk radiation makes a noticeable contribution in these regions.

Based on the analysis of the photometric and spectral data we have obtained, we can make the following conclusions about the structure and nature of the PGC 60020 galaxy.

1. PGC 60020 is a classical polar-ring galaxy. This is revealed by the features of its photometric structure, and, mainly, the presence of two kinematic subsystems, rotating in different planes. The diameter of the polar disk is not greater than the diameter of the main body of the galaxy, hence PGC 60020 belongs to the group of PRGs with the so-called inner polar rings (NGC 2685, IC 1689, AM 2020-504, etc.).

2. The main body of PGC 60020 is an S0 galaxy. This is confirmed by the analysis of the isophote shapes, and by decomposing the brightness profile into the components along the major axis (bulge + disk). The photometric characteristics of the main body, such as the absolute magnitude ($M_B = -19.^m9$), the parameters of the bulge and the disk ($h_d = 8.''2$ (4.7 kpc), $\mu_d = 21.9$ mag/arcsec²; $R_{e,b} = 1.''4$ (0.8 kpc), $\mu_{e,b} = 20.03$ mag/arcsec²), and the bulge-to-disk ratio (0.6) are typical of the S0 galaxies with polar rings [4, 23]. The estimate of the mass of the galaxy ($\geq 4.3 \times 10^{10} M_\odot$) and the mass-to-luminosity ratio ($\geq 6.8 M_\odot/L_\odot$) are also consistent with the above assertion.

3. The presence of emission lines ([NII] and H α) in the circumnuclear region of PGC 60020 suggests the ongoing activity of the galactic nuclei. The fact that the forbidden nitrogen line in this region is much brighter than the H α line is indicative of the gas emission from the shock ionization. In addition, the nitrogen line FWHM is about 460 km/s. The above data allow us to make an assumption that the nucleus of the PGC 60020 galaxy has the LINER? characteristics (see, e.g., [24]). However, the spectral observations in the blue region are yet required for the final conclusion.

4. Around the main body of the galaxy, in the plane inclined to the galactic plane by an angle of about 60° (our estimates), a disk, consisting of gas, stars and dust is rotating. The disk structure is very heterogeneous. The plane of the disk is inclined to the polar plane of the galaxy by an angle of about 30°.

5. A loop-like structure, possibly a tidal tail stretches from the southern part of the polar disk to the companion galaxy. However, it is currently unknown whether these galaxies do interact or we are simply observing a projection effect. If these galaxies are indeed close and interacting, the polar disk could be formed as a result of accretion of matter from the companion galaxy to PGC 60020.

6. The SDSS J171745.58+404137.1 galaxy is classified as E4–E5; red color indices and the absence of emission lines in its spectrum do not contradict this classification.

Acknowledgements

The authors are grateful to the Committee of Large Telescopes for allocating the observing time at the 6-m BTA telescope, and the staff of the SAO RAS, namely A. V. Moiseev for his help in the observations with the 6-m telescope, and I. D. Karachentsev for drawing our attention to the PGC 60020 galaxy as a possible PRG candidate. The initial work was supported by the Russian Foundation for Basic Research (grant no. 05-02-17548). O. A. Merkulova is also grateful to the support from the Federal target program Research and Pedagogical Cadre for Innovative Russia (no. 12.740.11.0133). The observations at the 6-m BTA telescope are performed with the financial support of the Ministry of Education and Science of the Russian Federation (state contracts no. 16.552.11.7028, 16.518.11.7073).

References

1. B. C. Whitmore, R. A. Lucas, D. B. McElroy, et al., *Astronom. J.* **100**, 1489 (1990).
2. K. Bekki, *Astrophys. J.* **499**, 635 (1998).
3. F. Bournaud and F. Combes, *Astronom. and Astrophys.* **401**, 817 (2003).
4. V. P. Reshetnikov and N. Ya. Sotnikova, *Astronom. and Astrophys.* **325**, 933 (1997).
5. E. Iodice, M. Arnaboldi, R. P. Saglia, et al., *Astrophys. J.* **643**, 200 (2006).
6. P. D. Sackett, H. Rix, B. J. Jarvis, and K. C. Freeman, *Astrophys. J.* **436**, 629 (1994).
7. F. Schweizer, B. C. Whitmore, and V. C. Ruben, *Astronom. J.* **88**, 909 (1983).
8. A. V. Moiseev, K. I. Smirnova, A. A. Smirnova, and V. P. Reshetnikov, *Monthly Notices Roy. Astronom. Soc.* **418**, 244 (2011).
9. G. M. Karataeva, O. A. Merkulova, A. N. Burenkov, in *VAK-2010 Conf. Proc.* (SAO RAS, Nizhnii Arkhyz, 2010), p. 127.
10. V. L. Afanasiev and A. V. Moiseev, *Astron. Lett.* **31**, 194 (2005).
11. A. U. Landolt, *Astronom. J.* **88**, 439 (1983).
12. S. I. Neizvestny, *Izvestiya SAO* **17**, 26 (1983).
13. J. Tonry and M. Davis, *Astronom. and Astrophys.* **84**, 1511 (1979).
14. G. M. Karataeva, I. O. Drozdovsky, V. A. Hagen-Thorn, et al., *Astronom. J.* **127**, 789 (2004).
15. V. V. Makarov, V. P. Reshetnikov and V. A. Yakovleva, *Astrofizika* **30**, 15 (1989).
16. V. P. Reshetnikov, V. A. Hagen-Thorn, and V. A. Yakovleva, *Astronom. and Astrophys.* **303**, 398 (1995).
17. R. I. Jedrzejewsky, *Monthly Notices Roy. Astronom. Soc.* **226**, 747 (1987).
18. R. F. Peletier, R. L. Davies, G. D. Illingworth, and L. E. Davis, *Astronom. J.* **100**, 1091 (1990).
19. R. Buta, S. Mitra, G. de Vaucouleurs, and H. G. Corwin, Jr., *Astronom. J.* **107**, 118 (1994).

20. D. J. Schlegel, D. P. Finkbeiner, and M. Davis, *Astrophys. J.* **500**, 525 (1998).
21. S. M. Kent, *Astrophys. J. Suppl.* **59**, 115 (1985).
22. V. A. Hagen-Thorn, L. V. Shalyapina, G. M. Karataeva, et al., *Astron. Rep.* **49**, 958 (2005).
23. V. P. Reshetnikov, *Astronom. and Astrophys.* **416**, 889 (2004).
24. S. Veilleux and D. E. Osterbrock, *Astrophys. J. Suppl.* **63**, 295 (1987).